compensate for the $q \approx 0$ acoustic modes.

RbCl is more complicated. The frequency shift and width clearly involve different combinations of anharmonic processes, since the width is changing rapidly at low temperatures in a region where the frequency is constant. This is similar to the behavior of the TO mode at $q = 0$ in AgBr.[8] However, the flattening out at high temperatures of the peak position is unusual and suggests a partial cancellation between competing anharmonic processes. It would be very interesting to see if this effect is observed by neutron scattering.

In conclusion, it appears that impurity-induced Raman scattering can be used to study anharmonic interactions in solids, and gives results in at least qualitative agreement with results obtained by more conventional techniques. The removal of translational symmetry allows the observation of phonons away from the zone center which can, otherwise, only be studied by the rather more cumbersome method of neutron scattering.

We are indebted to Dr. John B. Page, Jr., for many stimulating and informative sessions, to James Harrington and Indira Nair for assistance in taking the data, and to Dr. Lawrence B. Welsh for the loan of equipment.

*Work supported by the U.S. Army Research Office, Durham, N. C. and by the Advanced Projects Research Agency through the Northwestern University, Evanston, Ill., Materials Research Center.

[1]R. T. Harley, J. B. Page, Jr., and C. T. Walker, Phys. Rev. Letters 23, 922 (1969).

[2]J. B. Page, Jr., R. T. Harley, and C. T. Walker, Bull. Am. Phys. Soc. 15, 42 (1970).

[3]A. A. Maradudin and A. E. Fein, Phys. Rev. 128, 2589 (1962).

[4]G. Leibfried and W. Ludwig, in *Solid State Physics, Advances in Research and Applications*, edited by F. Seitz and D. Turnbull (Academic, New York, 1961), Vol. 12, p. 275.

[5]R. A. Cowley, Advan. Phys. 12, 421 (1963).

[6]A. D. B. Woods, W. Cochran, and B. N. Brockhouse, Phys. Rev. 119, 980 (1960); A. D. B. Woods, B. N. Brockhouse, R. A. Cowley, and W. Cochran, *ibid.* 131, 1025 (1963).

[7]A. S. Pine and P. E. Tannenwald, Phys. Rev. 178, 1424 (1969).

[8]G. O. Jones, D. H. Martin, P. A. Mawer, and C. H. Perry, Proc. Roy. Soc. (London) A261, 10 (1961).

[9]J. R. D. Copley, R. W. Macpherson, and T. Timusk, Phys. Rev. 182, 965 (1969).

[10]G. Raunio and L. Almqvist, Phys. Status Solidi 33, 209 (1969).

[11]M. Hass, Solid State Commun. 7, 1069 (1969).

[12]A. M. Karo, J. Chem. Phys. 33, 7 (1960).

[13]G. Raunio and S. Rolandson, Solid State Commun. 7, 1341 (1969).

[14]A. I. Stekhanov and A. P. Karol'kov, Fiz. Tverd. Tela 8, 920 (1966) [Soviet Phys. Solid State 8, 734 (1966)].

[15]G. K. White, Proc. Roy. Soc. (London) A286, 204 (1965).

PHYSICAL REVIEW B VOLUME 2, NUMBER 6 15 SEPTEMBER 1970

Impurity Raman Scattering from CaF_2:Ce

A. Kiel and J. F. Scott

Bell Telephone Laboratories, Holmdel, New Jersey 07733

(Received 28 April 1970)

We have investigated the scattering from CaF_2:Ce crystals in which part of the trivalent Ce impurities have been reduced to the divalent state. Although the Ce^{2+} concentration was extremely low (~ 10 ppm) we observe electronic Raman scattering. In addition, we have observed a defect-induced spectrum closely approximating the unperturbed one-phonon density of states. The latter scattering is due to phonon modulation of the impurity Rayleigh scattering.

I. INTRODUCTION

Crystalline materials containing a divalent cerium impurity have attracted considerable interest lately, partly because of the potentially useful photochromic properties of such substances.[1] An unusual feature of Ce^{2+} is the fact that in most solids the ground state appears to be a member of the $5d^1 4f^1$ manifold.[2] Very little is known about the low-lying states of Ce^{2+} in solid matrices since at the low concentrations available (< 0.01%), infrared absorption techniques lack sufficient sensitivity and EPR is masked by the large Ce^{3+} background from several sites. We therefore decided to study the electronic Raman scattering[3,4] from divalent Ce^{2+} in CaF_2 crystals. This method is often more sensitive than infrared methods,[4,5] and with the near resonance conditions (laser energy near the

absorption bands) which occur in Ce^{2+}, it was hoped that we could overcome the intensity limitations imposed by low concentrations. In one respect, CaF_2 is an almost ideal host; since only a single phonon of well-known frequency is Raman active, there can be no problem in interpreting the spectra.

Cerium is always doped into CaF_2 in the trivalent state, and it replaces a cation (calcium) substitutionally. Most of the cerium is associated with either a near-neighbor F^- interstitial or a near-neighbor divalent oxygen at a fluorine site.[1] However, a small part of the Ce^{3+} is not locally compensated so that its symmetry is $O_h(m3m)$. Since Ce^{3+} is nearly the same size as Ca^{2+}, little local distortion is expected. Trivalent cerium may be reduced to the divalent state by γ irradiation, uv irradiation, or by electrolytic means. All of the samples used in our experiments were additively colored and reduced with uv excitation. When rare earths in CaF_2 are reduced, it is found that the divalent ions reside at cubic (distantly compensated) sites.[6,7] This is not surprising since the locally compensated trivalent ions are certainly more stable and hence less likely to trap an electron than cubic (distantly compensated) ions. It is important to note that while the Ce^{3+} is an excellent fit at the Ca site, the Ce^{2+} is substantially larger than Ca^{2+}. [No published data on Ce^{2+} were available, but it is probable that $r(Ce^{2+}) - r(Ce^{3+}) \simeq 0.15-0.25$ Å.] It is perhaps surprising that no significant distortion[6] of the local symmetry results from the resulting size mismatch on reduction of rare earths. In any event, we expect the Ce (or any divalent rare earth) to be very tightly bound and not as well shielded from the lattice as is usual for the trivalent rare earths. We shall return to this point in Sec. IV.

II. MATERIALS AND EXPERIMENTAL SETUP

The experimental data were all obtained at temperatures between 6 and 10 °K, using an argon laser as a source. Several wavelengths of the laser were used for the scattering experiments. The trivalent state of Ce was reduced to the divalent state by illuminating with uv radiation from a 500-W mercury lamp for about 20–30 min prior to the collection of Raman data. Since the lifetime of the divalent cerium was but a few minutes at room temperature, it was necessary to activate the crystal while it was at liquid-helium temperatures. The cerium-doped CaF_2 crystals were all obtained from Kiss and Staebler of RCA Laboratories. The content of Ce^{3+} was about 0.01%. Observation of the absorption spectrum in the region of the characteristic $4f \rightarrow 5d$ Ce^{3+} lines indicates that about 5–10% of the trivalent ions[8] are reduced. We believe that this is the lowest concentration of any impurity detected by light scattering experiments (see, however, Worlock and Porto[9]).

Raman measurements were made by means of an argon laser which gave ~1 W at 4880 and 5145 Å, the two wavelengths principally used in these experiments. A Spex 1400 double monochromator, an EMI-6256 photomultiplier, and a Keithly 610B electrometer formed the rest of the detection system.

A serious problem in performing these experiments arose. The argon laser emission itself bleached the crystals and thus limited the time available for each spectral run to a few minutes. (We could not shift the beam to another part of the crystal very conveniently since there were few regions of adequate optical quality, and realignment of the spectrometer would have been required.) Working at longer wavelengths (> 6000 Å) to minimize bleaching was not feasible because of reduced scattering efficiency. This strong bleaching action is no doubt connected with the intensity of the interactions which caused the greatly enhanced scattering. In view of the 30-min activation time, the conditions for running this experiment were less than ideal, i.e., minutes of data acquisition per hour of working time was small.

III. EXPERIMENTAL RESULTS

All samples showed a single Raman line prior to uv irradiation, the T_{2g} mode at 325 cm^{-1} which is characteristic of CaF_2. After activation of the centers, additional features were observed in the 230–330 cm^{-1} (see Fig. 1) as well as the 1200–2000-cm^{-1} region (Fig. 2). Note that while the phonon line displays the expected selection rules (it disappears in xx polarization), no obvious selection rules occur in the other features. Checking these results with both 4880- and 5145-Å excitation conclusively shows that these features are not due to fluorescence. Indeed, there was no evidence of any fluorescence due to the Ce impurity.

The extra features proved to be substantially stronger when 4880-Å excitation was used than was the case with 5145-Å excitation.

The absorption spectrum of irradiated CaF_2:Ce is shown in Fig. 3 (taken from Ref. 8). The spectrum of the activated material is consistent with transitions from a $4f^15d^1(T_{2g})$ ground state to states of the $4f^2$ manifold (see Ref. 2 for detailed comparison of theory and experiment). The absorption line near 6000 Å is *not* believed to be due to a $4f^15d^1 \rightarrow 4f^2$ transition but may be a $4f^15d^1 \rightarrow 4d^2$ transition. It can be seen that the laser lines (4880 and 5145 Å) fall in a region where there is significant absorption. These lines are almost certainly due to several states with opposite parity

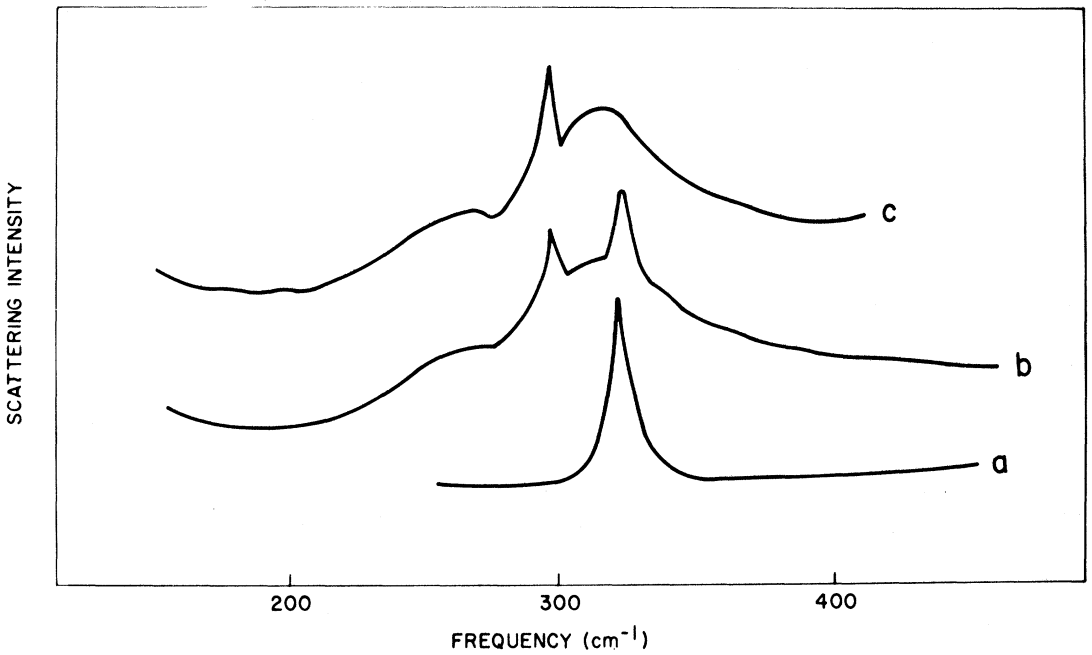

FIG. 1. Raman spectra of a CaF_2:Ce crystal in 200–400-cm^{-1} region: (a) xy polarization before uv activation; (b) xy polarization after uv activation; (c) xy polarization after uv activation. All data were taken at 8 °K. The T_{2g} phonon line is at 325 cm^{-1}.

from that of the ground state of Ce^{2+}. These states can act as intermediate states for a Raman transition, thus resulting in considerable resonant enhancement within the Ce^{2+} system.

Calculated energies for the $4f^15d^1$ states of Ce^{2+} in CaF_2 are contained in Ref. 2. The low-lying states (< 3000 cm^{-1}) are reproduced in Table I, together with observed features. We have calculated the *relative* Raman intensities[10] and included these in Table I.

In the region below 350 cm^{-1} (we will call this the very-low-frequency region) the agreement is poor not only in the position of the features but in the number observed. The frequencies of the features cannot be expected to be accurately predicted by the results of Alig *et al.*[2] since these authors simply did not have sufficient data to fix the parameters for the $4f^15d^1$ manifold. However, the magnitude of the errors in this region casts doubt on an electronic interpretation of these very-low-lying lines. Further discussion of these features will be given in Sec. IV.

In the region 1000–2400 cm^{-1}, we predict four moderately strong lines (1089, 1448, 1686, and 2404 cm^{-1}), and four are observed (1201, 1393, 1616, and 1940 cm^{-1}). The agreement of observed energy with that predicted in Ref. 2 is poor but we have already pointed out that this was to be expected. A number of weaker features were also observed in regions near predicted weak features. Using

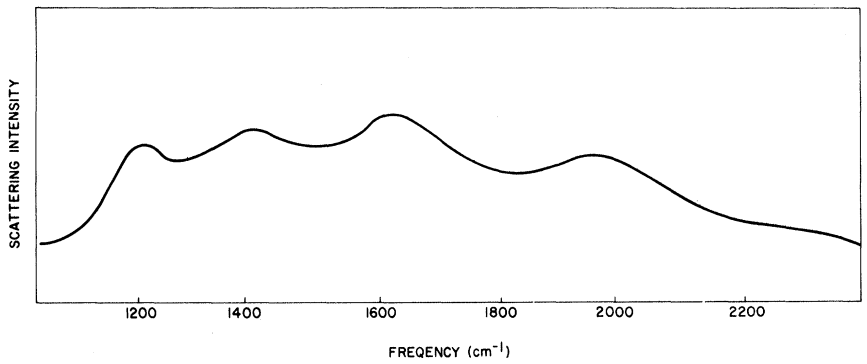

FIG. 2. Raman spectra of a CaF_2: Ce crystal in the 1200–2000-cm^{-1} region.

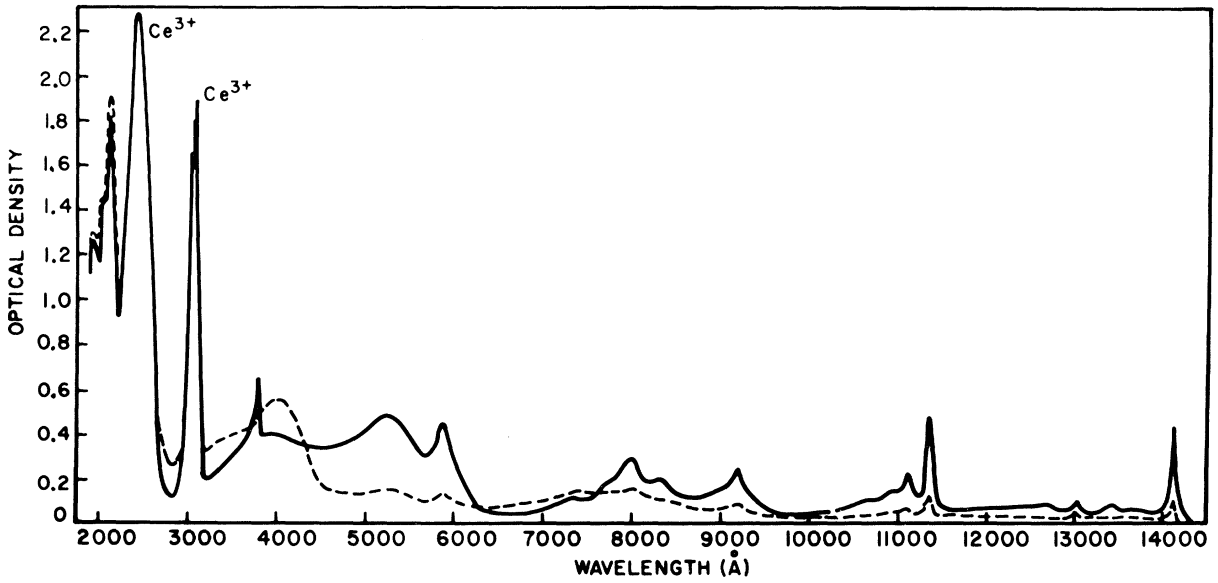

FIG. 3. Absorption spectrum of CaF_2:Ce. Solid lines: after activation; dashed lines: after activation *and* 5 min annealing at 100 °C. All spectra taken at 78 °K. The dashed spectrum was the same as the additive colored spectrum before uv activation.

these data, it may be possible to improve the crystal field calculations for the *fd* manifold; however, the lack of symmetry information from the Raman experiment makes that nontrivial.

The lack of any polarization selection rules in the defect scattering is not hard to understand. According to Ref. 2 the ground state is a T_{2g} state which is threefold degenerate. This state is very sensitive to crystal strain, which certainly must exist in the crystals, if for no other reason than the large size mismatch of Ce^{2+} at a Ca site. The large fluorine interstitial concentration is another source of substantial microscopic strain. Hence the Ce^{2+} site has a small deviation from cubic symmetry and there is a small random splitting of the threefold degeneracy. The result of this is that the right and left circular-polarization components are essentially independent and the *rectangular selection* rules are destroyed since these depend on the correlation between circular-polarization components. This is not an unusual situation; a small unresolved splitting due to a local magnetic field would also have just such an affect. This situation is a likely occurrence whenever the ground state of the system is degenerate (see Refs. 4 and 5 and the paper listed in Ref. 10). Note that the *normal selection rules* (i.e., σ, π) will still be observed in absorption.

We now summarize the situation regarding the features between 1200 and 2000 cm^{-1}. The factors consistent with an electronic interpretation are the following:

(a) The features are activated by uv irradiation.

(b) The selection rules suggest a degenerate ground state (as predicted for Ce^{2+} by Alig *et al.*[2]).

(c) There should be four "strong" lines in this region, and indeed four are observed.

(d) Although we do not strictly have "resonance scattering," there is a considerable amount of resonance enhancement such that Ce^{2+} scattering would be at least an order of magnitude greater than that of the more abundant Ce^{3+}.

The only uncertainties about this Ce^{2+} electronic Raman-effect interpretation of the spectra are relatively minor:

(i) The intensity of this spectrum is still somewhat greater than can easily be accounted for by resonance enhancement.

(ii) After a number of cycles (i.e., uv irradiation, laser bleaching, warming) the crystals seemed to change their properties and some results were difficult to reproduce. In particular, the bleaching rate increased considerably and background scatter increased. It is not clear that Ce^{2+} should behave in this way.

(iii) No line corresponding to the predicted strong line at 192 cm^{-1} was observed. However, if this line actually occurs at somewhat lower energy, it would have been obscured by the background scattering while at higher energy it may overlap the impurity mode scattering (see Sec. IV).

IV. IMPURITY MODE SCATTERING

We have already pointed out that the low-frequency features are essentially uncorrelated with the electronic spectrum predicted in Ref. 2.

TABLE I. Observed scattering features, calculated low-lying states (Ref. 2), and predicted scattering intensity (Ref. 9). The cubic representations are included in column 2.

Observed features (cm^{-1})	Calculated energy (cm^{-1})	Calculated relative intensity
	0 (T_{2g})	...
231–272	192 (E_g)	1.0
301	427 (T_{2g})	
315–325		
620 (weak, broad)		
960 (weak, broad)	1074 (A_{2g})	0.1
	1089 (T_{1g})	0.9
1201		
1393	1448 (E_g)	0.6
1505 (weak)	1686 (T_{1g})	1.8
1616	1837 (A_{1g})	0.12
1940	2116 (T_{2g})	0.1
2246 (weak)		
	2404 (A_{1g})	2.2
	2599 (T_{2g})	
	2644 (T_{1g})	

These features are similar to the high-frequency spectra in that they require uv activation, bleach at essentially the same rate as the high-frequency features, and evidence no polarization selection rules. As seen in Fig. 1, there appear to be two broad features and a sharper central feature. This behavior itself is most unusual for electronic spectra where the low-energy lines are usually the narrowest.

It has been suggested that[9] impurities can sometimes act as a probe for the pure phonons of the material. Recently, this has been demonstrated[11] for the case of Tl^- in KI, where phonon modes of the pure material were observed in Raman scattering; and in Ref. 12 phonon modes were observed in far-infrared absorption of NO_3^--doped KI. In a similar vein, the vibronic side bands associated with rare-earth impurity fluorescence in SrF_2 and $LaCl_3$ have also been used to study[13] the pure lattice phonon spectrum.

Elcombe and Pryor[14] have determined the acoustic-phonon spectrum of CaF_2 by fitting inelastic neutron scattering data with a shell model. In Fig. 4, we have superposed our low-frequency spectrum on the one-phonon density-of-states spectrum given in Fig. 3 of Ref. 14. The correlation is rather striking although not all of the features are reproduced. This figure may be compared with the similar results[15] obtained for infrared sidebands of H^- in CaF_2.

Our interpretation of these results is that the Ce^{2+} impurity centers are acting as scattering centers which are modulated by the phonon spectrum. In such a system, the scattering tensor will contain two terms, one due to Rayleigh scattering modulated by the phonons, and a second due to ordinary Raman scattering. In either case, the whole oscillator spectrum is displayed.[16] We believe that the very-low-frequency spectrum results from the electron-phonon interaction of Ce^{2+} with the lattice oscillators. This interaction will be at least an order of magnitude greater for the *fd* configuration of divalent Ce than is the case in the trivalent material. This results from the greater spatial extent of the *d* electron which can then "see" the lattice better. The enhanced lattice interaction of *d* electrons relative to *f* electrons is well known and is the reason why iron group ions will generally have crystal field splittings at least an order of magnitude greater than trivalent rare earths. The fact that the Ce is an impurity means that the $\vec{k}$ selection rules are relaxed and the entire phonon spectrum is observed. Note that the modulated defect term is nonzero owing to the breakdown of the $\vec{k}$ selection rule. It is important to note that the defect scattering effect we propose will be enhanced by the near resonance conditions, as can be seen from Eq. (2) below.

Another possible reason for the enhanced pho-

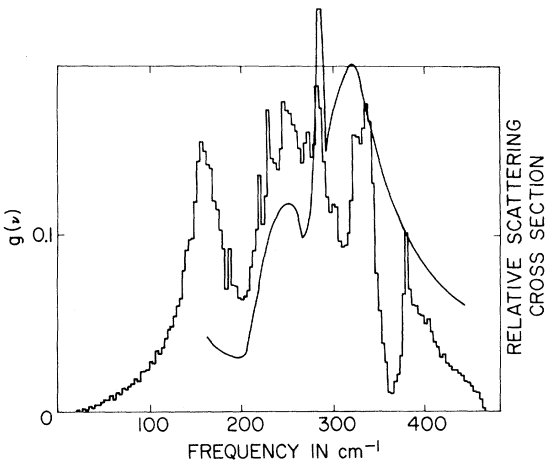

FIG. 4. Comparison of light scattering with shell-model calculation. The histogram is the one-phonon density of states and was reproduced from Ref. 14. The solid curve represents our light scattering data, as shown in Fig. 1.

non scattering in the divalent system is the fact that the divalent rare earths are all larger than Ca^{2+}. The radius of Ce^{2+} is at least 0.15–0.2 Å greater than Ca^{2+}. Since the restoring force goes as

$$k \simeq \exp(\delta r/\rho), \tag{1}$$

where ρ is the hardness parameter[17] (≈ 0.3 Å), the force constant for Ce^{2+} will be almost twice that of Ca^{2+} or Ce^{3+} and can therefore scatter phonons more efficiently. This increase in force constant has an important effect on the scattered light spectrum, which we discuss at the end of Sec. IV.

The description of the vibronic processes involved in the scattering is somewhat more complicated than the model used in Ref. 13. However, the results presented there can be generalized to cover our case. The power scattered includes a term independent of photon wavelength

$$P(\omega_p) = (4\pi I e^4/m^2c^4) f(\omega_p),$$

where I is the total laser intensity and $f(\omega_p)$ is a function describing the vibronic coupling. [It is to be understood that the frequency of the scattered light in $P(\omega_p)$ is *relative* to the laser frequency.] In the case of near resonance, this term is dominated by the more familiar type of expression

$$P(\omega_p) = \frac{4\pi\omega^4}{c^4} I \Big[\sum_i e^2 \left(\frac{1}{\triangle E_i - \hbar\omega} + \frac{1}{\triangle E_i + \hbar\omega} \right) \times | \langle \psi_{g,l} | x_\alpha | \psi_i \rangle \langle \psi_i | x_\beta | \psi_{g,m} \rangle | \Big]^2 h(\omega_p), \tag{2}$$

where E_i is the energy of the electronic intermediate state ψ_i, ω is the laser frequency (we are not taking into account the small difference in incident and scattered frequency) and $\psi_{g,l}$ is the lth component of the ground manifold.

The behavior of the function we have called $h(\omega_p)$ is discussed in Ref. 13. Under certain conditions (see pp. 263–264 of Ref. 13 and p. 522 of Ref. 18), we can write

$$h(\omega_p) = \frac{C}{\rho v_s^2} \left(a\omega_p + \frac{b}{\omega_p} \right) g(\omega_p), \tag{3}$$

where $g(\omega_p)$ is the density of states per unit frequency and volume; v_s is the sound velocity; ρ is the density; C, a, and b are constants (h, $a\omega_p$, and b/ω_p are dimensionless). The basic coupling constant in Eq. (3) is given by

$$h(\omega_p) \simeq \eta(\omega_p) \cdot g(\omega_p)$$

and

$$\eta(\omega_p) = \frac{C'}{\rho v_s^2} \frac{\omega_p}{(\triangle E)^2} .$$

The two terms in Eq. (3) (which is only approximate in its functional form) correspond to cases where $|\triangle E| = |E - E_i - \hbar\omega_p| > \hbar\omega_p$ (the $a\omega_p$ term) and $|\triangle E| = |E - E_i - \hbar\omega_p| < \hbar\omega_p$ (the b/ω_p resonant term).

If the $a\omega_p$ term dominates, the high-frequency end of the spectrum is enhanced, thus improving the agreement of our results with Elcombe and Pryor's work. Another reason for the enhancement of the high-frequency region follows from the discussion following Eq. (1). The increased force constant calculated for the Ce^{+2} system implies a decrease in the Raman intensity for low-frequency phonons and an increase for high-frequency oscillations. This is shown to be the case in Ref. 19.

V. SUMMARY

We have demonstrated the utility of resonant Raman scattering from very dilute solid solutions. In systems which exhibit no luminescence, such as that under consideration, this is the only method available for the determination of low-lying electronic level energies. Resonant scattering offers an additional advantage of selectivity: The ability to study Ce^{2+} centers in the present experiment, despite the greater numbers of Ce^{3+} ions, illustrates that virtue. It is clear that the dynamics of the $Ce^{3+} \rightarrow Ce^{2+}$ conversion in CaF_2, and other time-dependent processes, such as $Ce^{2+} \rightarrow Ce^{3+}$ bleaching, can be probed via this technique of resonant scattering. Application to photochromic processes involving doubly doped hosts is an obvious extension of the present work.

The strong defect-induced phonon scattering obtained shows that resonant scattering from impurities is a powerful method of obtaining one-phonon density-of-states data. Since most crystals are unavailable in sizes large enough for inelastic neutron scattering, this alternative source of such information is promising. The comparison of observed one-phonon scattering in $CaF_2:Ce^{2+}$ with that calculated from neutron data and a shell model shows that defect scattering is a useful measure of the unperturbed density of states. In materials which exhibit a strong second-order Raman spectrum, from which density-of-states information can be obtained, the defect-induced spectrum gives an independent check on the analysis, as shown by the recent KI studies.[11] What the present work shows is that less than 100 ppm of the right impurity is sufficient for such experimental measurements. It should not be difficult to dope most materials of interest to such levels.

ACKNOWLEDGMENTS

The authors would like to thank Miss M. El-

combe, A. W. Pryor, R. C. Alig, Z. Kiss, J. P. Brown, and D. S. McClure for allowing us to see the results of their work prior to publication and to reproduce parts of their papers. We are indebted to R. Staebler, Z. Kiss, and R. C. Alig for kindly supplying us with crystals and for some valuable advice. L. Cheesman's painstaking efforts with these difficult materials is humbly acknowledged.

---

[1]Z. J. Kiss, Phys. Today 23, 42 (1970); D. Staebler and Z. J. Kiss, Appl. Phys. Letters 14, 93 (1969).

[2]R. C. Alig, Z. J. Kiss, J. P. Brown, and D. S. McClure, Phys. Rev. 186, 276 (1969).

[3]J. A. Koningstein and O. S. Mortensen, in *Light Scattering Spectra of Solids*, edited by G. B. Wright (Springer, Berlin, 1969), p. 239 (further references to the work of these authors are contained in this paper).

[4]A. Kiel, Ref. 3, p. 245.

[5]A. Kiel and S. P. S. Porto, J. Mol. Spectry 32, 458 (1969).

[6]H. A. Weakliem and Z. J. Kiss, Phys. Rev. 157, 277 (1967).

[7]J. L. Merz and P. S. Pershan, Phys. Rev. 162, 217 (1967).

[8]D. Staebler (private communication).

[9]J. M. Worlock and S. P. S. Porto, Phys. Rev. Letters 15, 697 (1965).

[10]The procedure for calculating the Raman intensities is briefly described in A. Kiel, T. C. Damen, S. P. S. Porto, S. Singh, and F. Varsanyi, Phys. Rev. 178, 1518 (1969). The formalism of Ref. 2 was used in computing the reduced matrix elements. R. C. Alig kindly supplied us with the calculated wave functions.

[11]R. T. Harley, J. B. Page, and C. Walker, Phys. Rev. Letters 23, 922 (1969).

[12]R. K. Eijnthoven and J. van der Elsken, Phys. Rev. Letters 23, 1455 (1969).

[13]E. Cohen and H. W. Moos, Phys. Rev. 161, 258 (1967).

[14]M. Elcombe and A. W. Pryor, J. Phys. C 3, 492 (1970).

[15]R. J. Elliot, W. Hayes, G. D. Jones, H. F. Macdonald, and C. T. Sennett, Proc. Roy. Soc. (London) A289, 1 (1965).

[16]If the Ce^{2+} defects were ideally substitutional in a perfect lattice only the even-parity phonon spectrum would be displayed. The even-parity spectrum for CaF_2 is not available so that the fit of our spectrum to the complete spectrum of Ref. 14 cannot be expected to be perfect. To the extent that local F^- compensation and microscopic strain of the large C^{2+} ion are important, the parity selection rule will be relaxed. Note that the same selection rule holds in Ref. 15.

[17]M. Tosi, in *Solid State Physics*, edited by F. Seitz and D. Turnbull (Academic, New York, 1965), Vol. 16, p. 1.

[18]E. Cohen, L. A. Riseberg, and H. W. Moos, Phys. Rev. 175, 521 (1968).

[19]N. Xinh, A. A. Maradudin, and R. A. Coldwell-Horsfall, J. Phys. (Paris) 26, 717 (1965).